Since January 2020 Elsevier has created a COVID-19 resource centre with free information in English and Mandarin on the novel coronavirus COVID-19. The COVID-19 resource centre is hosted on Elsevier Connect, the company's public news and information website.

Virus Research 278 (2020) 197843

Contents lists available at ScienceDirect

Virus Research

journal homepage: www.elsevier.com/locate/virusres

Swine acute diarrhea syndrome coronavirus (SADS-CoV) antagonizes interferon-β production via blocking IPS-1 and RIG-I

Zhihai Zhou[a,b,1], Yuan Sun[a,b,1], Xiaoling Yan[a,b], Xiaoyu Tang[a,b], Qianniu Li[a,b], Yaorong Tan[a,b], Tian Lan[a,b,*], Jingyun Ma[a,b,*]

[a] College of Animal Science, South China Agricultural University, Guangzhou, China
[b] Key Laboratory of Animal Health Aquaculture and Environmental Control, Guangzhou, Guangdong, China

ARTICLE INFO

Keywords:
Swine acute diarrhea syndrome coronavirus
IPS-1
RIG-I
Interferon beta

ABSTRACT

Swine acute diarrhea syndrome coronavirus (SADS-CoV), a newly emerging enteric coronavirus, is considered to be associated with swine acute diarrhea syndrome (SADS) which has caused significantly economic losses to the porcine industry. Interactions between SADS-CoV and the host innate immune response is unclear yet. In this study, we used IPEC-J2 cells as a model to explore potential evasion strategies employed by SADS-CoV. Our results showed that SADS-CoV infection failed to induce IFN-β production, and inhibited poly (I:C) and Sendai virus (SeV)-triggered IFN-β expression. SADS-CoV also blocked poly (I:C)-induced phosphorylation and nuclear translocation of IRF-3 and NF-κB. Furthermore, SADS-CoV did not interfere with the activity of IFN-β promoter stimulated by IRF3, TBK1 and IKKε, but counteracted its activation induced by IPS-1 and RIG-I. Collectively, this study is the first investigation that shows interactions between SADS-CoV and the host innate immunity, which provides information of the molecular mechanisms underlying SASD-CoV infection.

1. Introduction

Swine acute diarrhea syndrome coronavirus (SADS-CoV), a newly discovered coronavirus, is an enveloped, positive and single-stranded sense RNA virus that belongs to the family Coronaviridae and the genus Alphacoronavirus (Gong et al., 2017; Pan et al., 2017; Zhou et al., 2018a). SADS-CoV is considered to be the causative agent of the fatal swine acute diarrhea syndrome (SADS) with clinical manifestations of severe, acute diarrhea and rapid weight loss in piglets, which caused significantly economic losses and seriously affected the development of the porcine industry in China (Gong et al., 2017; Pan et al., 2017; Zhou et al., 2018a). As a newly emerged coronavirus, recent researches of SADS-CoV have been mainly focused on clinical diagnosis, molecular epidemiology, evolution and animal models (Fu et al., 2018; Zhou et al., 2018a, b; Xu et al., 2019). To our knowledge, interactions between SADS-CoV and the host innate immune response is unknown, and detailed information on it is yet to be obtained.

The innate immunity is the first line of host defense against viral infections, and type I interferons (IFN), IFN-α/β, play important roles in the antiviral immune response. In the early stage of infection, host cells can recognize some conservative components of the virus, i.e. pathogen-associated molecular patterns, through pattern recognition receptors including Toll-like receptors and RIG-I-like receptors. Following recognition, specific signal pathways of these receptors are activated to induce expressions of type I interferons. Then the type I interferon binds to its receptor to activate downstream JAK/STAT1 signaling pathway, which ultimately produces a series of interferon-stimulating factors that can inhibit the virus proliferation (Kawai and Akira, 2006; Carlos et al., 2007; Li et al., 2010). For most RNA viruses, double-stranded RNA (dsRNA) is the replicative intermediate, which is mainly recognized by

Abbreviations: CPE, cytopathic effect; dsRNA, double-stranded RNA; IFA, indirect immunofluorescence assay; IFN-β, interferon beta; IPEC-J2, porcine small intestinal epithelial cells; IPS-1, mitochondria antiviral-signaling protein; IRF-3, IFN regulatory factor 3; IKKε, inhibitor of κB kinase-ε; MDA5, melanoma differentiation-associated gene 5; MERS-CoV, Middle East respiratory syndrome coronavirus; MOI, multiplicity of infection; mRNA, messenger RNA; NF-κB, nuclear factor-kappaB; PAMPs, pathogen-associated molecular patterns; PBS, phosphate buffered saline; PEDV, porcine epidemic diarrhea virus; p.i., post-infection; poly(I:C), polyinosinic-polycytidylic acid; PRRs, pattern recognition receptors; qRT-PCR, quantitative real time RT-PCR; RIG-I, retinoic acid-inducible gene I; RT-PCR, reverse transcription polymerase chain reaction; SADS-CoV, swine acute diarrhea syndrome coronavirus; SARS-CoV, severe acute respiratory syndrome coronavirus; SeV, Sendai virus; TBK1, TANK-binding kinase 1; TGEV, transmissible gastroenteritis virus; TLR3, toll-like receptor 3

* Corresponding authors at: College of Animal Science, South China Agricultural University, Guangzhou, China.
E-mail addresses: lantian2016@scau.edu.cn (T. Lan), majy2400@scau.edu.cn (J. Ma).
[1] These authors contributed equally to this work.

https://doi.org/10.1016/j.virusres.2019.197843
Received 9 August 2019; Received in revised form 10 December 2019; Accepted 18 December 2019
Available online 26 December 2019

retinoic acid-inducible gene I (RIG-I) and melanoma differentiation-associated gene 5 (MDA5) (Andrejeva et al., 2004; Cao et al., 2015).

To antagonize the host innate immune response, coronaviruses have developed various strategies to evade defenses and successfully infected host cells. Porcine epidemic diarrhea virus (PEDV) interacted with IPS-1 to inhibit IFN-β transcription in porcine small intestinal epithelial cells (Cao et al., 2015). Porcine deltacoronavirus (PDCoV) suppressed IFN-β production by blocking the activation of transcription factors IRF3 and NF-κB in a porcine kidney cell line, LLC-PK1 cells (Luo et al., 2016). Although Transmissible gastroenteritis virus (TGEV) infection didn't suppress IFN-β induction, it induced a delayed activation of the IFN response in IPEC-J2 cells (Zhu et al., 2017a). Severe acute respiratory syndrome coronavirus (SARS-CoV) interfered with IRF-3 function to prevent activation of the innate immune system in VeroE6 and human 293 cells (Spiegel et al., 2005). Mouse hepatitis virus (MHV) employed unique strategies to circumvent the IFN-α/β response at multiple steps, such as causing an inhibition of IFN-β production at a posttranscriptional level (Roth-Cross et al., 2007). Porcine reproductive and respiratory syndrome virus (PRRSV) suppressed production of IFN-β by interfering with the IPS-I activation in the RIG-I signaling pathway (Luo et al., 2008). Compared with these knowledge, there is an urgent need to revel evasion strategies employed by SADS-CoV infection to provide meaningful information for virus control.

In this study, we investigated interactions between SADS-CoV infection and the host innate immune response for the first time. Intestinal porcine epithelial cells (IPEC-J2) was used as an infection model to determine the underlying molecular mechanism of SADS-CoV infection. Our results clearly showed that SADS-CoV infection failed to activate IFN-β expression and inhibited poly (I:C) and Sendai virus (SeV)-induced IFN-β production. SADS-CoV infection interrupted the RIG-I signaling pathway via inactivation of IPS-1 and RIG-I to impede the activation of IRF3 to inhibit the expression of IFN-β.

2. Materials and methods

2.1. Viruses, cells, and reagents

The strain SADS-CoV/CN/GDGL/2017 (Genbank accession number MG605090), isolated from a suckling piglet with the acute diarrhea in Guangdong Province of China in 2017, was used in this study with the $TCID_{50}$ of $10^{7.25}$/mL. The porcine intestinal columnar epithelial cells (IPEC-J2) kindly donated by Guangdong Wen's Group Academy of Sciences were cultured in Dulbecco's modified Eagle's medium (DMEM) supplemented with 10 % fetal bovine serum (FBS) and incubated at 37 °C in a humidified 5 % CO_2. Polyinosinic-polycytidylic acid [poly (I:C)] used as positive control was purchased from Invivogen (USA) and dissolved in water to obtain a stock solution of 1 mg/mL. Sendai virus (SeV) was kindly donated by Wuhan Institute of Virology, Chinese Academy of Sciences. The Dual-Luciferase® Reporter Assay System was purchased from Promega Corporation (Madison, WI, USA) and monoclonal β-actin antibody was purchased from Abbkine (Abbkine, Catalog: abm40032, USA). Anti-IRF-3, anti-phosphorylated IRF-3 (p-IRF-3) and anti-NF-κB, anti-phosphorylated NF-κB (p-NF-κB) rabbit monoclonal antibodies and horseradish peroxidase (HRP)-conjugated anti-rabbit IgG were purchased from Absin Bioscience, Inc. (Shanghai, China). Goat anti-mouse IgG/Alexa Fluor 488 antibody, goat anti-mouse IgG/Alexa Fluor 488 antibody and goat anti-rabbit IgG/Alexa Fluor 594 antibody were purchased from Bioss (Beijing, China). Anti-SADS-CoV N protein polyclonal antibody were obtained from BALB/c mice immunized with SADS-CoV N recombinant protein expressed by the plasmid pET-32a (+)-N, which was able to specifically react with SADS-CoV.

2.2. Plasmids

The standard plasmids DNA for the real-time RT-PCR assay were used with methods described by Zhou et al. (2018b). The plasmids IFN-β-Luc for IFN-β and Renilla luciferase construct pRL-TK were kindly donated by Dr. Shaobo Xiao (Huazhong Agricultural University, Wuhan, Hubei Province, China). The pCNA3.1-RIG-I recombinant expression plasmid were kindly provided by Dr. Shijun Zheng (China Agricultural University, Beijing, China). Porcine IPS-1, IKKε, TBK1 and IRF3 were cloned into pCNA3.1-3xHA. These plasmids were constructed by the TianYi HuiYuan company (TianYi HuiYuan, Wuhan, China).

2.3. Luciferase reporter gene assay

When the confluency reaching approximately 70%–80% in 24-well plates, IPEC-J2 cells were co-transfected with the reporter plasmid (IFN-β-Luc) of 0.2 μg/well and the plasmid pRL-TK (an internal control for normalization of the transfection efficiency) of 0.1 μg/well with Lipofectamine 3000 reagent. Then cells were mock-infected or infected by SADS-CoV at a multiplicity of infection (MOI) of 1. After 24 h, cells were treated with or without poly (I:C) (1.0 μg) or SeV as positive control for additional 12 h. Or IPEC-J2 were infected or mock-infected with SADS-CoV for 12 h prior to transfection of the luciferase reporter plasmids alone or co-transfection with the indicated expression plasmids (0.5 μg). Harvested cells were lysed and the firefly luciferase and Renilla luciferase activities were determined with the Dual-Luciferase reporter assay system (Promega) according to the manufacturer's protocol. Data were expressed as the relative firefly luciferase activities normalized to Renilla luciferase activities from three independently conducted experiments.

2.4. RNA extraction and quantitative real-time RT-PCR

IPEC-J2 cells were mock-infected or infected with SADS-CoV (MOI = 1), and cells transfected with poly (I:C) were used as positive control. Or IPEC-J2 cells were infected by SADS-CoV (MOI = 1) or mock infected for 24 h, and finally infected or mock-infected by SeV for addition 12 h. Total RNA was extracted from the transfected cells using TRIzol reagent (Invitrogen, USA) and reverse-transcribed into complementary DNA (cDNA) by using PrimeScript™ RT reagent Kit with gDNA Eraser (Takara, Biotechnology, Dalian, China). The cDNA was then used as the template in a SYBR green PCR assay (Genstar, Biotechnology, Beijing, China) with specific primer pairs targeting IFN-β and β-actin (Table 1). The abundance of the individual mRNA transcript in each sample was assayed for three times and normalized to that of β-actin mRNA (the internal control). The TaqMan-based real-time qPCR assay established by Zhou et al. (2018b) was employed to detect SADS-CoV genome copies.

2.5. ELISA assay for IFN-β protein

IPEC-J2 cells were mock-infected or infected with SADS-CoV at a MOI of 1. At 24 h post infection, cells were treated or not treated with SeV for additional 12 h. The supernatants were then harvested for an ELISA assay with a porcine IFN-β detection kit according to the

Table 1
Primers and probe used for real-time RT-PCR.

Primers	Sequence (5,-3,)	References
IFN-β	F:ACCAACAAAGGAGCAG R:TTTCATTCCAGCCAGT	(Zhang et al., 2017)
β-actin	F:GACATCAAGGAGAAGCTGTGC R:TGAAGGTAGTTTCGTGGATGC	(Zhang et al., 2017)
SADS-CoV-N	F:CTGACTGTTGTTGAGGTTAC R:TCTGCCAAAGCTTGTTTAAC	(Zhou et al., 2018b)
probe	5, -FAM -TCACAGTCTCGTTCTCGCAATCA-TAMRA-3,	(Zhou et al., 2018b)

manufacturer's instructions (Cusabio, Wuhan, China).

2.6. Indirect immunofluorescence assay (IFA)

IPEC-J2 cells were cultured in laser confocal dishes. When the confluency reaching 70 %–80 %, cells were mock-infected or infected with SADS-CoV at a MOI of 1. At 12 h post infection (hpi), cells were transfected with 2.0 μg of poly (I:C) or left untransfected. Another 12 h later, cells were fixed with 4 % paraformaldehyde for 10 min and then permeated with 0.1 % Triton X-100 for 10 min at room temperature. After three washes with PBS, cells were sealed with PBS containing 5 % bovine serum albumin (BSA) for 1 h and then incubated separately with rabbit polyclonal antibody against IRF3 (1:200) and mouse monoclonal antibody against the SADS-CoV-N (1:200) for 1 h at room temperature. Then cells were processed with Alexa Fluor secondary antibody for 1 h followed by 4′,6-diamidino-2-phenylindole-dihydrochloride (DAPI) for 15 min at room temperature. After washing with PBS, cells were examined with the confocal laser scanning microscope (Leica SPE; Leica, Germany) to collect fluorescent images.

2.7. Western blot analysis

IPEC-J2 cells cultured in 6-well plates were mock-infected or infected with SADS-CoV at a MOI of 1 or treated with poly (I:C) for the indicative times, lysed in RIPA Lysis Buffer (Boytime) supplemented with a proteases inhibitor cocktail and boiled for 10 min. The lysates were separated by 10 % sodium dodecyl sulfate-polyacrylamide gel electrophoresis (SDS-PAGE) and transferred onto Immobilon-P membrane (EMD Millipore, Billerica, MA, USA). After blocking with 5 % BSA, the membrane was incubated with rabbit monoclonal antibodies against IRF-3, p-IRF-3, NF-κB, p-NF-κB, HA at room temperature for 1 h, followed by incubation with horseradish peroxidase (HRP)-conjugated anti-rabbit IgG (1:10,000) for 30 min at room temperature. An anti-SADS-CoV N protein polyclonal antibody was used to confirm the expression levels of the SADS-CoV N protein. Expression of β-actin was detected with an anti-β-actin mouse monoclonal antibody to confirm loading of equal protein amounts. Protein blots were detected using an enhanced chemiluminescence (ECL) detection system and an Azure c600 visible fluorescent western blot imaging system (Azure Biosystems, America).

2.8. Statistical analysis

Unless otherwise indicated, all data were shown as mean ± SEM of independent experiments performed in triplicate. SPSS statistics 22 (International Business Machines Corporation, America) was used for statistical analyses. Comparisons between groups were considered statistically significant at $p < 0.05$. Student's *t*-test was used to determine statistical significance and *P*-values of < 0.05 were considered statistically significant.

3. Results

3.1. SADS-CoV proliferation characteristics in IPEC-J2 cells

In this study, IPEC-J2 cells were infected with SADS-CoV/CN/GDGL/2017 at a 1 MOI. Infected cells were monitored by IFAs using a polyclonal antibody against SADS-CoV N protein at 12, 24, 36, 48 hpi. As shown in Fig. 1A, only a small number of fluorescent signals were detected at 12 hpi. While at 24 hpi, more cells with obviously cytopathic effects were detected positive for SADS-CoV, indicating that viruses began to proliferate rapidly in IPEC-J2 cells. Along with cell detachment occurring, fluorescence signals began to weaken at 36 hpi. No obvious proliferation of SADS-CoV was detected after 48 hpi due to a large number of monolayer cells exfoliation. As the same time, the genome copies of SADS-CoV were detected by the TaqMan-based real-time qPCR assay. The results showed that the number of genome copies exhibited a gradually upward tendency before 12 hpi, and increased rapidly after 12 hpi. At 36 hpi, the number of SADS-CoV genome copies reached the highest level and then decreased after 36 hpi. Congruent with the result of qPCR, the western blot analysis of SADS-CoV N protein also showed that the level of N protein increased with the time of infection. And at 36 hpi, the amount of N protein reached the highest level, and same with that at 48 hpi (Fig.1). Taken together, SADS-CoV infection in IPEC-J2 cells gained the high genomic copies without cell detachment at 24 hpi, which provided a reference for in *vitro* studies of SADS-CoV infection.

3.2. SADS-CoV infection failed to induce IFN-β expression and inhibited poly (I:C) or SeV-mediated IFN-β production

To investigate whether SADS-CoV infection can induce IFN-β production in IPEC-J2 cells, the mRNA expression, the promoter activity and the protein level of IFN-β were analyzed after SADS-CoV infection. As shown in Fig. 2A, the mRNA expression of IFN-β was hardly detected at all indicated time points in SADS-CoV-infected cells, while the poly (I:C)-transfected cells used as the positive control presented remarkable expressions of IFN-β mRNA, especially on 9 hpi and 12 hpi. Similarly, another positive control SeV also induced the mRNA expression of IFN-β in mock-infected cells infected with SeV. However, in SADS-CoV infected cells, the IFN-β mRNA mediated by SeV was obviously inhibited (Fig. 2B). For the IFN-β promoter luciferase activity analysis, IPEC-J2 cells were first transfected with the luciferase reporter system including the IFN-β-Luc luciferase reporter plasmids and the internal control plasmid pRL-TK, then followed by infection with SADS-CoV (MOI = 0.1; MOI = 1), mock-infection, and poly (I:C) (1 μg/well), respectively. Similar to the result of the IFN-β mRNA expression, the IFN-β luciferase activity was also barely detectable in SADS-CoV infected IPEC-J2 cells compared with the strong signal in cells transfected with poly (I:C) (Fig. 2C). To further identify whether SADS-CoV can inhibit poly (I:C)-or SeV induced IFN-β promoter activity, IPEC-J2 cells were co-transfected with IFN-β-Luc and pRL-TK, then infected by SADS-CoV (MOI = 1) or mock infected for 12 h, and finally either transfected with or without poly (I:C), or infected or mock infected by SeV for addition 12 h. As shown in Fig. 2D, the activation of IFN-β promoter induced by poly(I:C) was obviously blocked in SADS-CoV-infected cells compared with mock-infected cells transfected with poly(I:C). Similar to Fig. 2D, SeV infection also significantly increased the activity of IFN-β promoter. While in SADS-CoV-infected cells, IFN-β promoter activity induced by SeV was inhibited by the virus (Fig. 2E). The protein expression of IFN-β was also detected. Congruent with the mRNA and the promoter activity of IFN-β, the protein expression induced by SeV was also inhibited by SADS-CoV (Fig. 2 F). Taken together, these results indicated that SADS-CoV infection failed to activate IFN-β production and inhibited poly (I:C) or SeV-triggered IFN-β activity.

3.3. SADS-CoV inhibited poly (I:C)-induced phosphorylation and nuclear translocation of IRF-3 and NF-κB

To determine the inhibitory mechanism of SADS-CoV on IFN induction in IPEC-J2 cells, the activation of IRF3 and NF-κB was identified after SADS-CoV infection. As shown in Fig. 3A, levels of IRF-3 and NF-κB proteins in SADS-CoV transfected cells were similar with those in mock-infected cells. Compared with the amount of p-IRF-3 and p-NF-κB detected in poly (I:C) transfected cells, p-IRF-3 and p-NF-κB showed a very low level of expression in SADS-CoV infected cells, and the expression of these two molecules mediated by poly (I:C) were obviously inhibited by SADS-CoV infection. The relative luciferase activities of IRF-3 and NF-κB were also measured. As shown in Fig. 3B, compared with the luciferase promoter activity in mock-infected cells, a little decrease of IRF3 activity and no change of NF-κB activity were observed in SADS-CoV inoculated cells. Both IRF3 and NF-κB activity

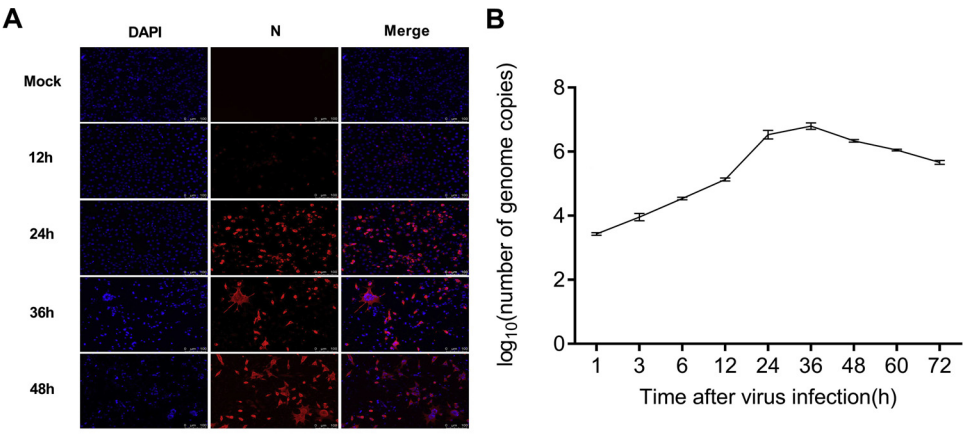

Fig. 1. SADS-CoV proliferation characteristics in IPEC-J2 cells. (A) IPEC-J2 cells were mock-infected or infected with SADS-CoV (MOI = 1). At 12, 24, 36, 48 hpi, the cells were fixed and incubated with a polyclonal antibody against SADS-CoV N protein (red). Fluorescent images were acquired with a confocal microscopy, ×20 (Leica, Wetzlar, Germany). (B) IPEC-J2 cells were mock-infected or infected with SADS-CoV (MOI = 1). At 1, 3, 6, 12, 24, 36, 48, 60, 72 hpi, viral copies were determined by TaqMan-based real-time RT-PCR assay and represented as mean ± SD with three replicates. (C) IPEC-J2 cells were mock-infected or infected with SADS-CoV (MOI = 1). At 12, 24, 36, 48 hpi, cell extracts were prepared and subjected to western-blot analysis.

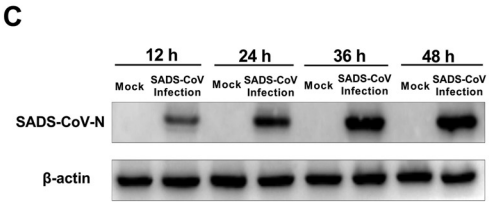

induced by poly (I:C) were obviously inhibited by SADS-CoV infection. Moreover, the nuclear translocation of IRF-3 and NF-κB were analyzed through the confocal microscopy assay. As shown in Fig. 3C and 3D, the nucleus translocation of IRF3 and NF-κB significantly reduced in SADS-CoV transfected cells in comparison to mock-infected cells transfected with poly (I:C). Meanwhile, SADS-CoV prevented the nuclear translocation of IRF3 and NF-κB induced by poly(I:C). In a word, these results clearly showed SADS-CoV inhibited the activation of IRF-3 and NF-κB.

3.4. SADS-CoV failed to block IRF3, TBK1 and IKKε activity

Previous studies indicate that the coronavirus mainly interacts on the RIG-I signaling pathway to interrupt IFN expression (Likai et al., 2019; Zhu et al., 2017b; Luo et al., 2016). As mentioned above, IRF3 activity showed a little decrease in SADS-CoV infected cells, there is a possibility that SASD-CoV infection may act on IRF3 to inhibit INF-β expression. To address this problem, IPEC-J2 cells were mock-infected or infected by SADS-CoV at a MOI of 1, and then co-transfected with IFN-β promoter luciferase reporter and over-expression plasmids of IRF3 to detect IFN-β activity. As shown in Fig. 4A, the IFN-β promoter activity in SADS-CoV infected cells was same with that in mock-infected cells, suggesting that SADS-CoV infection did not directly interrupt the activity of IRF3, and the target molecules of SADS-CoV infection may localize the upstream of IRF3 in the RIG-I signaling pathway.

To further identify the potential target for SASD-CoV infection, TBK1 and IKKε, two essential kinases for IRF-3 activation, were analyzed in IPEC-J2 cells after SADS-CoV infection. SADS-CoV infected and mock-infected cells were co-transfected with IFN-β-Luc and over-expression plasmids of TBK1 and IKKε. The results showed that the IFN-β promoter activity was activated in both infected and mock-infected cells, which indicated that SADS-CoV failed to block TBK1 and IKKε activity (Fig. 4B). Results here suggested that the molecules targeted by SADS-CoV were still in the upstream of TBK1 and IKKε.

3.5. SADS-CoV impeded IFN-β induction mediated by IPS-1 and RIG-I

IPS-1 is located upstream of TBK and IKKε in the RIG-I signaling pathway. Hence, the IFN-β promoter luciferase activity was analyzed with IPS-1 over-expressing in SADS-CoV infected or mock-infected IPEC-J2 cells. The result showed that in SADS-CoV-infected cells, IPS-1-mediated IFN-β luciferase activity (1.87-fold) was lower than that in mock-infected cells (3.22-fold) (Fig. 5A), which was obviously different from the effect of TBK and IKKε. This result indicated that IPS-1 may be the target protein for SADS-CoV infection in the RIG-I signaling way. Considering that IPS-1 is an adapter molecule of RIG-I, the RIG-I-induced IFN-β activity may also be inhibited. To confirm this speculation, mock infected or SADS-CoV-infected IPEC-J2 were transfected with RIG-I over-expression plasmid as well as the IFN-β promoter luciferase reporter plasmid. As shown in Fig. 5B, similar to the effect of IPS-1, RIG-I-induced IFN-β promoter activity was obviously inhibited by SADS-CoV infection in IPEC-J2 cells (1.7-fold) compared with that in mock-infected cells (3-fold). Taken together, the results showed that SADS-CoV interacted with IPS-1 and RIG-I to block IFN-β production.

4. Discussion

In this study, we explored interactions between SADS-CoV infection and the host innate immune for the first time. Previous studies revealed remarkable villus atrophy and severe pathological lesions in intestines of SADS-CoV inoculated piglets, indicating that the primary target cells of SASD-CoV in *vivo* are intestinal epithelial cells, which is same with other porcine enteric coronaviruses, PEDV and PDCoV (Zhou et al., 2018a; Xu et al., 2019; Koonpaew et al., 2019; Wang et al., 2019). Intestinal epithelium plays an important role in the intestinal mucosa immune response against pathogens (Temeeyasen et al., 2018). In order to yield relevant biological information consistent with in *vivo* SADS-CoV infection, we employed IPEC-J2 cells as a model to investigate molecular mechanisms underlying SADS-CoV infection. Our results showed that similar to PEDV, PDCoV and PPRSV (Luo et al., 2008; Cao et al., 2015; Luo et al., 2016), SADS-CoV did not induce IFN-β production and inhibited poly(I:C) or SeV-mediated IFN-β expression, which suggested that this may play a crucial role for the pathogenesis of these viruses.

The activity of IRF3 and NF-κB are essential for IFN-β production, and meanwhile TBK1 and IKKε are required to activate IRF3 and NF-κB (Iwamura et al., 2001; Hacker and Karin, 2006). Thus, these important molecules are aimed by coronaviruses with different mechanisms to inhibit IFN-β production. For instance, through blocking the IRF3

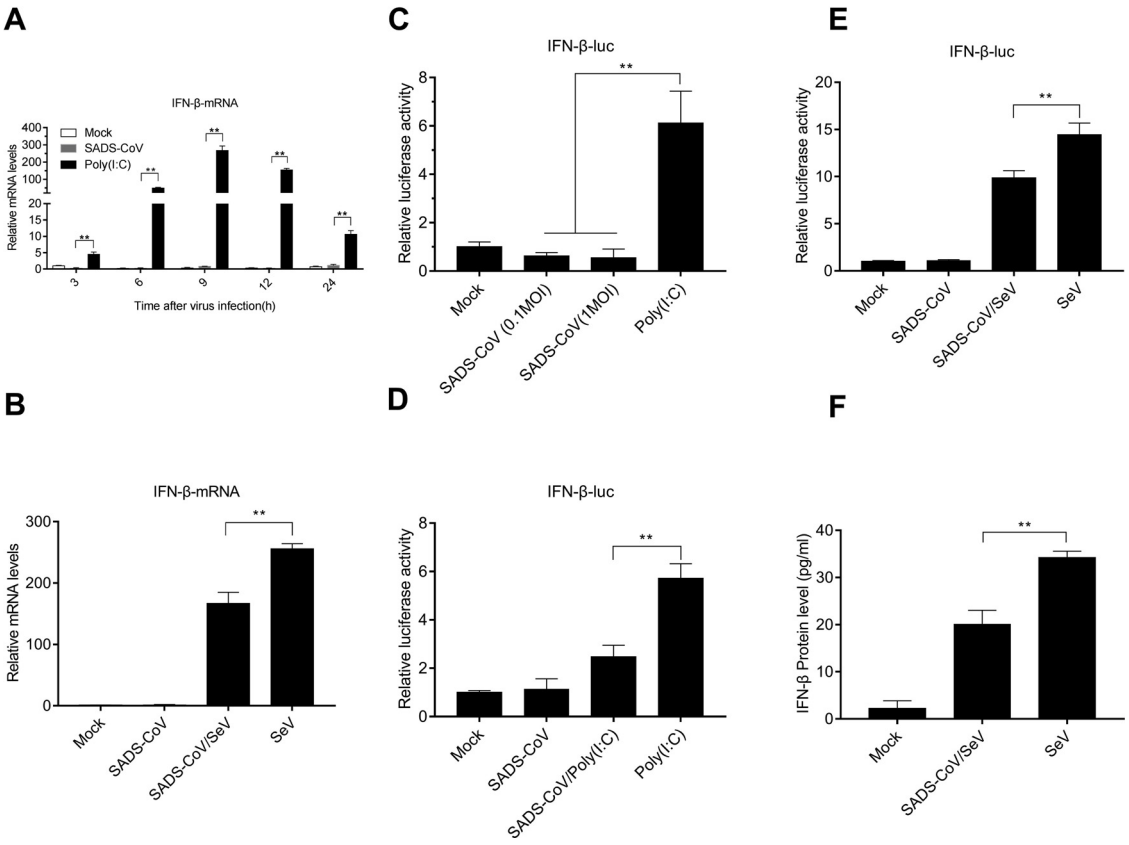

Fig. 2. SADS-CoV does not induce IFN-β production and inhibits poly (I:C)-induced IFN-β transcription. (A) IPEC-J2 cells were mock-infected or infected with SADS-CoV (MOI = 1). Cells transfected with poly (I:C) were used as positive control. At 3, 6, 9, 12, 24 hpi, total RNA was extracted to determine relative mRNA expression of IFN-β by real-time RT-PCR assay. The mRNA level of IFN-β were normalized to mRNA level of GAPDH. (B) IPEC-J2 cells were infected or mock infected with SADS-CoV (MOI = 1 or 0.1) for 24 h, the cells were treated or not treated with SeV for addition 12 h. Total RNA was extracted to determine relative mRNA expression of IFN-β by real-time RT-PCR assay. (C) IPEC-J2 cells were co-transfected with IFN-β-Luc and phRL-TK, and then infected with SADS-CoV (MOI = 1 or 0.1) for 24 h. Cells transfected with poly (I:C) for additional 12 h were used as positive control. (D and E) IPEC-J2 cells were co-transfected with IFN-β-Luc and phRL-TK, and then infected with SADS-CoV (MOI = 1 or 0.1) for 24 h. Then cells were treated or not treated with poly(I:C) (D) or SeV (E) for addition 12 h. Relative activity of IFN-β promoter was determined by dual-luciferase assay. (F) IPEC-J2 cells were mock mock-infected or infected with SADS-CoV at a MOI of 1. At 24 hpi, cells were treated or not treated with SeV for 12 h. The supernatants were then harvested for an ELISA analysis with a porcine IFN-β detection kit. All data were represented as mean ± SD with three replicates. *, $p < 0.05$; **, $p < 0.01$.

phosphorylation by the membrane protein, the middle east respiratory syndrome coronavirus (MERS-CoV) could suppress the type I interferon expression (Lui et al., 2016). The nonstructural protein (NSP) 5 encoded by PDCoV inhibited IFN-β production through the cleavage of NEMO, which was responsible for the recruitment of TBK1 and IKKε and the activation of IKK complex (Zhu et al., 2017b). In our study, the phosphorylation and nuclear translocation of IRF3 were interrupted by SADS-CoV infection, but IRF3, TBK1 and IKKε over-expression increased the IFN-β promoter activity in SADS-CoV inoculated cells, which indicated that SADS-CoV didn't target these signal molecules.

Activating TBK1 and IKKε needs interactions between IPS-1 and RIG-I, so we further investigated the roles of IPS-1 and RIG-I in SADS-CoV infections. The results showed that contrary to the enhance of the IFN-β promoter activity induced by TBK1 and IKKε, the IFN-β promoter activity associated with IPS-1 and RIG-I over-expression was blocked by SADS-CoV infection. This suggested that SADS-CoV may target IPS-1 to block IFN-β production. PEDV and PRRSV also interfered with IPS-1 activation to inhibit the production of IFN-β (Luo et al., 2008; Cao et al., 2015). RIG-I is also the aim for many coronaviruses. The nucleocapsid proteins of MHV and SARS-CoV antagonist IFN-β by attenuation of PACT-mediated RIG-I activation (Ding et al., 2017). The accessory protein NS6 encoded by PDCoV antagonized IFN-β production by interfering with the binding of RIG-I to double-stranded RNA (Fang et al., 2018).

SADS-CoV, PEDV and PDCoV are three emerging and highly pathogenic enteric coronaviruses in pigs in China (Wang et al., 2019). As a newly identified porcine enteric coronavirus, SADS-CoV seemed to share similarities on interactions with the host innate immune with PEDV and PDCoV (Table 2). Both SADS-CoV and PDCoV blocked the phosphorylation and nuclear translocation of IRF3 and NF-κB, but PEDV interrupted IRF3 not NF-κB. While, some other research showed that NSP1 of PEDV interfered the phosphorylation and degradation of IκBα and thus blocked NF-κB activation (Zhang et al., 2017). Furthermore, SADS-CoV and PEDV failed to block the activity of TBK1 and IKKε, but inhibited the activity of IPS-1 and RIG-I. We also noticed that SADS-CoV blocked the mRNA expressions of IFN-β, IRF3, TBK1, IKKε, IPS-1 and RIG-I (data not shown). Previous results suggested that coronaviruses can degrade cellular mRNA and inhibit protein synthesis (Fung et al., 2016; de Wilde et al., 2018). Future researches are needed to better understand the evasion strategies utilized by SADS-CoV, for example, roles of structural or nonstructural proteins encoded by SADS-CoV in the viral evasion mechanisms, and the antagonistic effects to host TLR signal pathway or the IFN-mediated JAK/STAT1 signal pathway.

5. Conclusions

In summary, this is the first time to reveal the molecular mechanism utilized by SADS-CoV to antagonize the host innate immune responses. Our results showed that SADS-CoV infection did not induce IFN-β

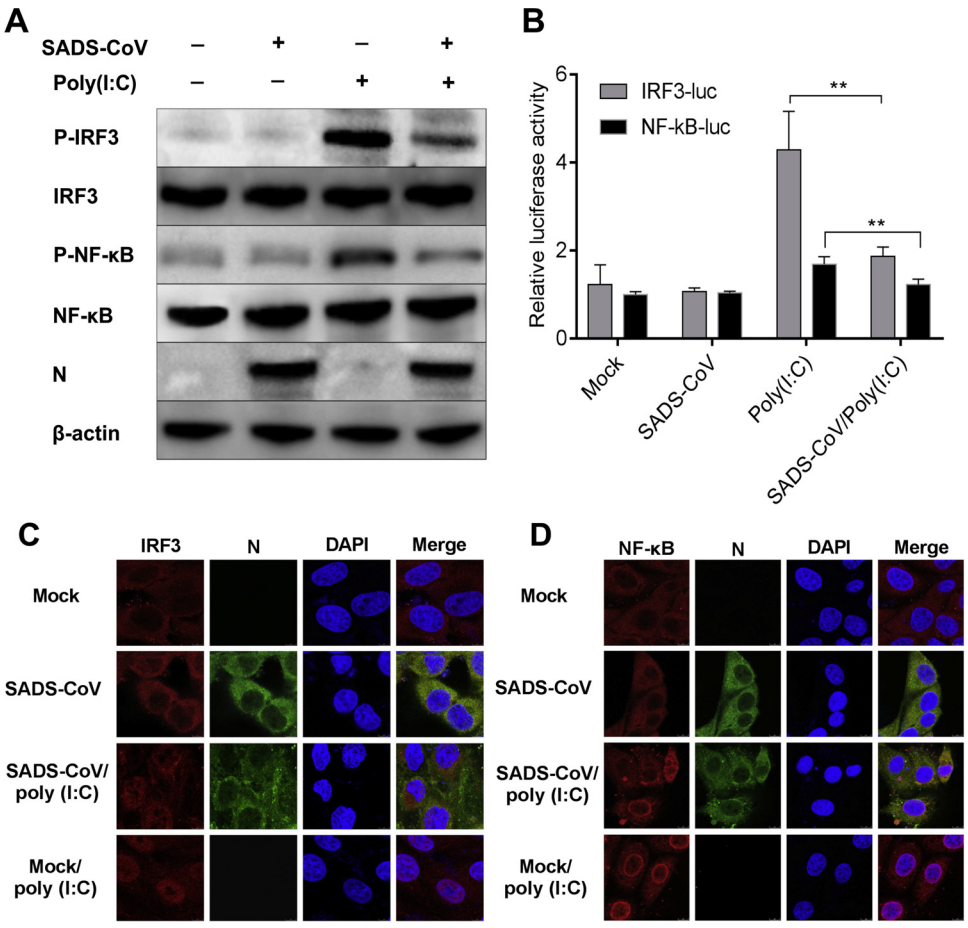

Fig. 3. SADS-CoV inhibits poly (I:C)-mediated IRF-3 and NF-κB activation. (A) IPEC-J2 cells were mock-infected or infected with SADS-CoV (MOI = 1) for 12 h, or treated with poly (I:C) for additional 12 as positive control. Cell extracts were prepared and subjected to western-blot analysis with specific antibodies for IRF-3, p-IRF-3, NF-κB, p-NF-κB or SADS-CoV N protein. Anti-β actin was used as a control for sample loading. Experiment that was repeated three times. (B) IPEC-J2 cells were infected or mock-infected with SADS-CoV (MOI = 1) for 12 h, and then co-transfected with pIRF3-Luc/ pNF-κB-Luc and phRL-TK for 12 h. Cells transfected with poly (I:C) for additional 12 h were used as positive control. Relative activity of IRF3/NF-κB promoter in IPEC-J2 cells was determined by dual-luciferase assay at 36 hpi. All data were expressed as means ± SD of three independent experiments. (C) and (D) IPEC-J2 cells were infected or mock-infected with SADS-CoV (MOI = 1) for 12 h, and then transfected with or without poly (I:C) for additional 12 h. At 24 hpi, cells were fixed with 4 % paraformaldehyde and 0.1 % Triton X-100 and stained by DAPI (blue). Cells were analyzed by a confocal laser scanning microscope (Leica SPE; Leica, Germany) to detect IRF3 (C) (red) or NF-κB (D) (red) and SADS-CoV N protein (green) singals. All data were represented as mean ± SD of three replicates. *, $p < 0.05$; **, $p < 0.01$.

production in IPEC-J2 cells. SADS-CoV primarily interfered with the activity of IPS-1 and RIG-I to inhibit the phosphorylation and nuclear translocation of IRF3 to block the IFN-β production. Further understanding of SADS-CoV-mediated IFN antagonists would help yield therapeutic targets to control viral infection.

Funding

This work was supported by the Research and Extension of Major Animal Epidemic Prevention and Control Technologies in the Strategic Project of Rural Revitalization of Guangdong Agricultural Department of China (Building Modern Agricultural System) (2018-2020), the Science and Technology Program of Guangzhou City of China (No. 201904010433), and China Scholarship Council (201807630021).

CRediT authorship contribution statement

Zhihai Zhou: Data curation, Formal analysis, Investigation, Validation, Visualization, Writing - original draft. **Yuan Sun:** Formal analysis, Writing - original draft, Writing - review & editing. **Xiaoling**

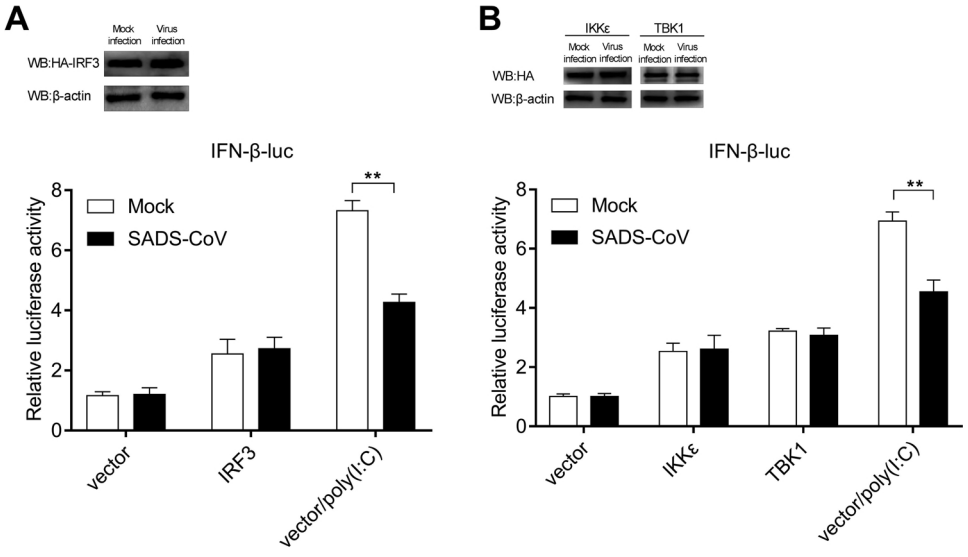

Fig. 4. SADS-CoV failed to block the activity of IRF3, TBK1 and IKKε. IPEC-J2 cells were mock-infected or infected with SADS-CoV (MOI = 1) for 12 h, and then co-transfected with IFN-β promoter luciferase reporter and over-expression plasmids of IRF3 (A), TBK1 and IKKε (B) or an empty vector for 12 h. IPEC-J2 cells transfected with poly (I:C) were used as positive control. Relative activity of IFN-β promoter in IPEC-J2 cells was determined by dual-luciferase assay or cell extracts were prepared and subjected to western-blot analysis. All data were represented as mean ± SD of three replications. *, $p < 0.05$; **, $p < 0.01$.

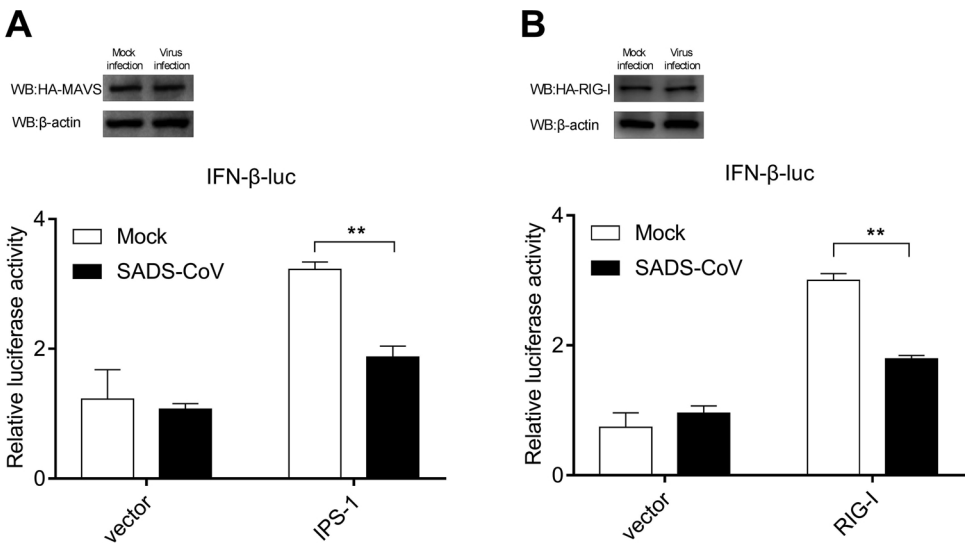

Fig. 5. SADS-CoV impeded IFN-β induction mediated by IPS-1 and RIG-I. IPEC-J2 cells were mock-infected or infected with SADS-CoV (MOI = 1), and then co-transfected with IFN-β-Luc and over-expression plasmids of IPS-1 (A), RIG-I (B), or an empty vector for 24 h. Relative activity of IFN-β promoter in IPEC-J2 cells was determined by dual-luciferase assay or cell extracts were prepared and subjected to western-blot analysis. All data were represented as mean ± SD of three replications. *, $p < 0.05$; **, $p < 0.01$.

Table 2
Summary of interactions between three enteric coronaviruses or PRRSV and the host innate immune response.

	PEDV	SADS-CoV	PDCoV	PRRSV
IFN-β production	○/×	○/×	○/×	○/×
Phosphorylation and nuclear translocation of IRF-3	○/×	○/×	○/×	○/×
Phosphorylation and nuclear translocation of NF-κB	↑/√	○/×	○/×	no information
IRF3-mediated IFN-β production	no information	○	↓	○
TBK1/IKKε-mediated IFN-β production	○	○	↓	○
IPS-1-mediated IFN-β production	↓	↓	↓	↓
RIG-I-mediated IFN-β production	↓	↓	↓	↓
MDA5-mediated IFN-β production	on information	no information	↓	no information
Target molecules	IPS-1	IPS-1 and RIG-I	IRF3	IPS-1
Reference	Cao et al., 2015		Luo et al., 2016	Luo et al., 2008

↓: significant decline.
↑: higher than mock.
○: same as mock.
√: induce.
×: inhibit.

Yan: Data curation. **Xiaoyu Tang:** Investigation. **Qianniu Li:** Validation. **Yaorong Tan:** . **Tian Lan:** Resources, Supervision, Conceptualization. **Jingyun Ma:** Funding acquisition, Project administration, Supervision, Conceptualization, Resources.

Declaration of Competing Interest

The authors declare no conflict of interests with any organization.

Acknowledgments

The authors would like to acknowledge Professor Shaobo Xiao from Huazhong Agricultural University for his donation of experimental materials.

References

Andrejeva, J., Childs, K.S., Young, D.F., Carlos, T.S., Stock, N., Goodbourn, S., Randall, R.E., 2004. The V proteins of paramyxoviruses bind the IFN-inducible RNA helicase, mda-5, and inhibit its activation of the IFN-beta promoter. Proc. Natl. Acad. Sci. U. S. A. 101, 17264–17269. https://doi.org/10.1073/pnas.0407639101.

Cao, L., Ge, X., Gao, Y., Herrler, G., Ren, Y., Ren, X., Li, G., 2015. Porcine epidemic diarrhea virus inhibits dsRNA-induced interferon-beta production in porcine intestinal epithelial cells by blockade of the RIG-I-mediated pathway. Virol. J. 12, 127. https://doi.org/10.1186/s12985-015-0345-x.

Carlos, T.S., Young, D., Stertz, S., Kochs, G., Randall, R.E., 2007. Interferon-induced inhibition of parainfluenza virus type 5; the roles of MxA, PKR and oligo A synthetase/RNase L. Virology 363, 166–173. https://doi.org/10.1016/j.virol.2007.01.014.

de Wilde, A.H., Snijder, E.J., Kikkert, M., van Hemert, M.J., 2018. Host factors in coronavirus replication. Curr. Top. Microbiol. Immunol. 419, 1–42. https://doi.org/10.1016/j.coviro.2018.12.001.

Ding, Z., Fang, L., Yuan, S., Zhao, L., Wang, X., Long, S., Wang, M., Wang, D., Foda, M.F., Xiao, S., 2017. The nucleocapsid proteins of mouse hepatitis virus and severe acute respiratory syndrome coronavirus share the same IFN-beta antagonizing mechanism: attenuation of PACT-mediated RIG-I/ MDA5 activation. Oncotarget 8, 49655–49670. https://doi.org/10.18632/oncotarget.17912.

Fang, P., Fang, L., Ren, J., Hong, Y., Liu, X., Zhao, Y., Wang, D., Peng, G., Xiao, S., 2018. Porcine deltacoronavirus accessory protein NS6 antagonizes interferon Beta production by interfering with the binding of RIG-I/MDA5 to double-stranded RNA. J. Virol. 92. https://doi.org/10.1128/JVI.00712-18.

Fu, X., Fang, B., Liu, Y., Cai, M., Jun, J., Ma, J., Bu, D., Wang, L., Zhou, P., Wang, H., Zhang, G., 2018. Newly emerged porcine enteric alphacoronavirus in southern China: Identification, origin and evolutionary history analysis. Infect. Genet. Evol. 62, 179–187. https://doi.org/10.1016/j.meegid.2018.04.031.

Fung, T.S., Liao, Y., Liu, D.X., 2016. Regulation of stress responses and translational control by coronavirus. Viruses 8. https://doi.org/10.3390/v8070184.

Gong, L., Li, J., Zhou, Q., Xu, Z., Chen, L., Zhang, Y., Xue, C., Wen, Z., Cao, Y.A., 2017. New Bat-HKU2-like coronavirus in swine, China, 2017. Emerg. Infect. Dis. 23, 1607–1609. https://doi.org/10.3201/eid2309.170915.

Hacker, H., Karin, M., 2006. Regulation and function of IKK and IKK-related kinases. Sci. STKE 2006 (357), re13. https://doi.org/10.1126/stke.3572006re13.

Iwamura, T., Yoneyama, M., Yamaguchi, K., Suhara, W., Mori, W., Shiota, K., Okabe, Y., Namiki, H., Fujita, T., 2001. Induction of IRF-3/-7 kinase and NF-kappaB in response to double-stranded RNA and virus infection: common and unique pathways. Genes Cells 6, 375–388. https://doi.org/10.1046/j.1365-2443.2001.00426.x.

Kawai, T., Akira, S., 2006. Innate immune recognition of viral infection. Nat. Immunol. 7, 131–137. https://doi.org/10.1038/ni1303.

Koonpaew, S., Teeravechyan, S., Frantz, P.N., Chailangkarn, T., Jongkaewwattana, A., 2019. PEDV and PDCoV Pathogenesis: The Interplay Between Host Innate Immune Responses and Porcine Enteric Coronaviruses. Front. Vet. Sci. 6, 34. https://doi.org/10.3389/fvets.2019.00034.

Likai, J., Shasha, L., Wenxian, Z., Jingjiao, M., Jianhe, S., Hengan, W., Yaxian, Y., 2019. Porcine deltacoronavirus nucleocapsid protein suppressed IFN-beta production by

interfering porcine RIG-I dsRNA-Binding and K63-Linked polyubiquitination. Front. Immunol. 10, 1024. https://doi.org/10.3389/fimmu.2019.01024.

Li, J., Liu, Y., Zhang, X., 2010. Murine coronavirus induces type I interferon in oligodendrocytes through recognition by RIG-I and MDA5. J. Virol. 84, 6472–6482. https://doi.org/10.1128/JVI.00016-10.

Lui, P.Y., Wong, L.Y., Fung, C.L., Siu, K.L., Yeung, M.L., Yuen, K.S., Chan, C.P., Woo, P.C., Yuen, K.Y., Jin, D.Y., 2016. Middle East respiratory syndrome coronavirus M protein suppresses type I interferon expression through the inhibition of TBK1-dependent phosphorylation of IRF3. Emerg. Microbes Infect. 5, e39. https://doi.org/10.1038/emi.2016.33.

Luo, J., Fang, L., Dong, N., Fang, P., Ding, Z., Wang, D., Chen, H., Xiao, S., 2016. Porcine deltacoronavirus (PDCoV) infection suppresses RIG-I-mediated interferon-beta production. Virology 495, 10–17. https://doi.org/10.1016/j.virol.2016.04.025.

Luo, R., Xiao, S., Jiang, Y., Jin, H., Wang, D., Liu, M., Chen, H., Fang, L., 2008. Porcine reproductive and respiratory syndrome virus (PRRSV) suppresses interferon-beta production by interfering with the RIG-I signaling pathway. Mol. Immunol. 45, 2839–2846. https://doi.org/10.1016/j.molimm.2008.01.028.

Pan, Y., Tian, X., Qin, P., Wang, B., Zhao, P., Yang, Y., Huang, Y., 2017. Discovery of a novel swine enteric alphacoronavirus (SeACoV) in southern China. Vet. Microbiol. 211, 15–21.

Roth-Cross, J.K., Martinez-Sobrido, L., Scott, E.P., Garcia-Sastre, A., SR, Weiss, 2007. Inhibition of the alpha/beta interferon response by mouse hepatitis virus at multiple levels. J. Virol. 81, 7189–7199. https://doi.org/10.1128/JVI.00013-07.

Spiegel, M., Pichlmair, A., Martinez-Sobrido, L., Cros, J., Garcia-Sastre, A., Haller, O., Weber, F., 2005. Inhibition of Beta interferon induction by severe acute respiratory syndrome coronavirus suggests a two-step model for activation of interferon regulatory factor 3. J. Virol. 79, 2079–2086. https://doi.org/10.1128/JVI.79.4.2079-2086.2005.

Temeeyasen, G., Sinha, A., Gimenez-Lirola, L.G., Zhang, J.Q., Pineyro, P.E., 2018. Differential gene modulation of pattern-recognition receptor TLR and RIG-I-like and downstream mediators on intestinal mucosa of pigs infected with PEDV non S-INDEL and PEDV S-INDEL strains. Virology 517, 188–198. https://doi.org/10.1016/j.virol.2017.11.024.

Wang, Q., Vlasova, A.N., Kenney, S.P., Saif, L.J., 2019. Emerging and re-emerging coronaviruses in pigs. Curr. Opin. Virol. 34, 39–49. https://doi.org/10.1016/j.coviro.2018.12.001.

Xu, Z., Zhang, Y., Gong, L., Huang, L., Lin, Y., Qin, J., Du, Y., Zhou, Q., Xue, C., Cao, Y., 2019. Isolation and characterization of a highly pathogenic strain of Porcine enteric alphacoronavirus causing watery diarrhoea and high mortality in newborn piglets. Transbound. Emerg. Dis. 66, 119–130. https://doi.org/10.1111/tbed.12992.

Zhang, Q., Ma, J., Yoo, D., 2017. Inhibition of NF-kappaB activity by the porcine epidemic diarrhea virus nonstructural protein 1 for innate immune evasion. Virology 510, 111–126. https://doi.org/10.1016/j.virol.2017.07.009.

Zhou, L., Sun, Y., Wu, J.L., Mai, K.J., Chen, G.H., Wu, Z.X., Bai, Y., Li, D., Zhou, Z.H., Cheng, J., et al., 2018b. Development of a TaqMan-based real-time RT-PCR assay for the detection of SADS-CoV associated with severe diarrhea disease in pigs. J. Virol. Methods 255, 66–70. https://doi.org/10.1016/j.jviromet.2018.02.002.

Zhou, P., Fan, H., Lan, T., Yang, X.L., Shi, W.F., Zhang, W., Zhu, Y., Zhang, Y.W., Xie, Q.M., Mani, S., et al., 2018a. Fatal swine acute diarrhoea syndrome caused by an HKU2-related coronavirus of bat origin. Nature 556, 255–258. https://doi.org/10.1038/s41586-018-0010-9.

Zhu, L., Yang, X., Mou, C., Yang, Q., 2017a. Transmissible gastroenteritis virus does not suppress IFN-beta induction but is sensitive to IFN in IPEC-J2 cells. Vet. Microbiol. 199, 128–134. https://doi.org/10.1016/j.vetmic.2016.12.031.

Zhu, X., Fang, L., Wang, D., Yang, Y., Chen, J., Ye, X., Foda, M.F., Xiao, S., 2017b. Porcine deltacoronavirus nsp5 inhibits interferon-beta production through the cleavage of NEMO. Virology 502, 33–38. https://doi.org/10.1016/j.virol.2016.12.005.